

Selected Paper

Microwave-Assisted Synthesis of Monodisperse Nickel Nanoparticles Using a Complex of Nickel Formate with Long-Chain Amine Ligands

Tomohisa Yamauchi,[1] Yasunori Tsukahara,*[1] Tetsuo Sakamoto,[2] Takumi Kono,[2] Makoto Yasuda,[3] Akio Baba,[3] and Yuji Wada*[4]

[1]Graduate School of Engineering, Osaka University, 2-1 Yamada-oka, Suita 565-0871

[2]Nippon Steel Chemical Co., Ltd., 14-1 Sotokanda 4-chome, Chiyoda-ku, Tokyo 101-0021

[3]Department of Applied Chemistry, Graduate School of Engineering, Osaka University, 2-1 Yamada-oka, Suita 565-0871

[4]Department of Applied Chemistry, Graduate School of Science and Engineering, Tokyo Institute of Technology, 2-12-12 Ookayama, Meguro-ku, Tokyo 152-8552

Received March 19, 2009; E-mail: ytsuka@jrl.eng.osaka-u.ac.jp, yuji-w@apc.titech.ac.jp

We have successfully prepared face-centered cubic (fcc) Ni nanoparticles by the intramolecular reduction of Ni^{2+} ion contained in a formate complex having long-chain amine ligands within an extremely short time under microwave irradiation. Formate ion coordinated to Ni^{2+} ion acted as a reducing agent for Ni^{2+} in this reaction and finally decomposed to hydrogen and carbon dioxide. Ligation of the long-chain amine lowered the reaction temperatures by decreasing the energy barrier required for the reduction of the nickel formate complex. Monodisperse Ni nanoparticles with average sizes of 43, 71, and 106 nm were prepared using the complex of nickel formate with several chain lengths of alkylamines such as oleylamine (=(*Z*)-9-octadecenylamine), myristylamine (=tetradecylamine), and laurylamine (=dodecylamine), respectively. The relationship between the magnetic properties and the particle sizes of Ni nanoparticles is discussed.

Nanoparticles of ferromagnetic metals such as Fe, Co, and Ni have been extensively studied for catalysts, permanent magnets, magnetic fluids, and magnetic recording media.[1–9] Their physical and chemical properties depend on their sizes and shapes.[10–12] Among these metals, Ni nanoparticles have attracted much attention in application to conductive adhesives and electrodes in multilayer ceramic capacitors,[13–15] because of low cost than silver nanoparticles and high chemical stability compared to copper nanoparticles. Recently, unagglomerated pure Ni nanoparticles for technological applications are required to have fine particle sizes between 50–100 nm with a narrow size distribution as well as high crystallinity, because nanoparticles with sizes below 20 nm suffer from low oxidation resistance and nanoparticles with sizes over 100 nm have a problem of low dispersibility. Therefore, a number of physical and chemical techniques have been developed to produce Ni nanoparticles.

The reactions in gas–solid phases such as chemical vapor deposition of $NiCl_2$,[16] frequently induce agglomeration of the produced particles, leading to Ni particles having large sizes between submicro- and micrometer scales. Several solution-phase reactions such as sonochemical deposition,[17] microemulsion synthesis,[18] several chemical reduction methods,[19–23] polyol methods,[24–29] and hydrothermal reactions,[30] have been studied to produce fine particles. In these solution-phase methods, monodispersed Ni nanoparticles having small sizes between a few nanometers and 50 nm were obtained by adding surface modifying agents. Both phase methods have displayed difficult problems in preparing monodispersed Ni particles with sizes in the middle range between 50 nm and several hundred nanometers. A new process is desired for preparation of Ni nanoparticles having sizes between 50–100 nm.

Now we have selected the intramolecular reduction of nickel formate dihydrate to avoid adding other toxic reducing agents for the synthesis of Ni nanoparticles. Ni particles have been prepared by thermal decomposition of a neat formate salt at temperatures above 523 K.[31–34] In the intramolecular reduction method using nickel formate dihydrate, formate ion acted as a reducing agent for Ni^{2+} and finally decomposed to hydrogen and carbon dioxide according to the following reactions.

$$2HCOO^- \rightarrow 2CO_2 + H_2 + 2e^-$$
$$Ni^{2+} + 2e^- \rightarrow Ni^0 \quad (1)$$

This pyrolytic synthesis gave Ni powders with a wide size distribution in the micrometer range in spite of the molecular level reduction of Ni^{2+} ion producing Ni atom in the initial stage of the reaction. The large particle sizes obtained in this method could be attributed to aggregation of the particles while the reaction system was heated at high temperatures. Our strategies employed for controlling the particle sizes were as described below: 1) The reaction should be carried out in reduced concentration of the precursor using a solvent to decrease the collision frequencies of Ni^0 nuclei. 2) The particle sizes can be controlled by adding surface modifying agents to prevent excess particle growth. 3) The reaction temperature should be lowered. Then we have applied the ligation of nickel formate with alkylamines in order to change the geometric and electronic structures of the complex.

Reactants are directly heated under microwave irradiation through the interaction of the oscillating electric and magnetic

Published on the web August 7, 2009; doi:10.1246/bcsj.82.1044

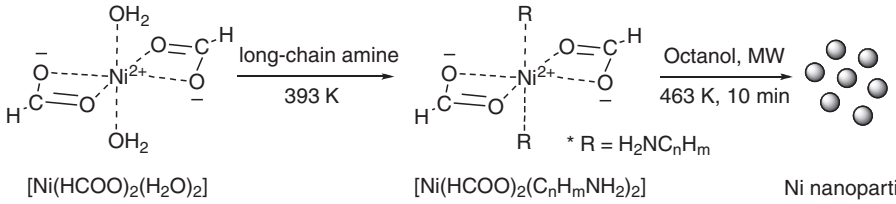

Scheme 1. Synthesis of Ni nanoparticles using nickel formate complex with long-chain amine ligands.

fields with substances and are quickly and uniformly heated. Therefore, nucleus growth should simultaneously and homogeneously occur in the entire vessel and particles with a narrow size distribution can be obtained within a short time.[35–37] Recently, preparation of monodispersed Ag and Cu nanoparticles with a narrow size distribution has been demonstrated by using microwave-assisted alcohol reduction.[38–40] Wada et al. and Tsuji et al. reported that cubic or spherical Ni nanoparticles with narrow size distribution (7 or 6 nm) were rapidly prepared by the polyol method under microwave irradiation through reduction of $Ni(OH)_2$ with ethylene glycol with or without using Pt catalyst as a nucleation agent, respectively.[41,42] We have selected a microwave-assisted method for the preparation of Ni nanoparticles in this work.

Combination of the above-described three strategies and the microwave method has enabled preparation of fcc Ni nanoparticles having the desired particle sizes by the intramolecular reduction of Ni^{2+} ion contained in its formate complex with long-chain amine ligands within a short time at 463 K. The sizes of the obtained particles were controlled using various long-chain amine ligands. The coordination environment of Ni^{2+} ion should be changed by ligation with the long-chain amines to nickel formate, enhancing the reactivity of the complex.

Experimental

Materials. Nickel formate dihydrate, 1-octanol, and tetraethylene glycol (=bis[2-(2-hydroxyethoxy)ethyl] ether) were purchased from Kishida Chemical Co., Ltd. Laurylamine and myristylamine were purchased from Tokyo Chemical Industry Co., Ltd. Oleylamine was purchased from Aldrich Co., Ltd. These reagents were used as supplied.

Preparation of Ni Complex $[Ni(HCOO)_2(C_{12}H_{25}NH_2)_2]$. The complex of $[Ni(HCOO)_2(C_{12}H_{25}NH_2)_2]$ was prepared from nickel formate dihydrate (1 mmol) and laurylamine (10 mmol) in chloroform (20 mL) under heating at 393 K for 20 min. The reaction solution changed from a greenish suspending solution to a deep green homogeneous solution. While cooling to room temperature, the color of the solution changed to turquoise blue. The reaction solution was left at rest. After several weeks, blue crystals were collected. Elemental analysis was performed with a YANAKO CHN coder MT-5 (YANAKO). Analytical data: Calcd for $C_{26}H_{56}N_2O_4Ni$: C, 60.12; H, 10.87; N, 5.39%. Found: C, 59.87; H, 10.69; N, 5.25%.

Preparation of Ni Nanoparticles. Microwave heating was carried out by using a multi-mode 2.45 GHz microwave apparatus at 770 W (μ Reactor, Shikoku Instrumentation Co., Ltd.). The temperatures of the reaction solution were measured with a fiber-optic thermometer (AMOTH TM-5886, Anritsu Meter Co., Ltd.) directly inserted into the solution. The agitation control was carried out at an agitation speed of 200 rpm with an agitator motor (EYELA MAZALA-Z, Tokyo Rikakikai Co., Ltd.) equipped with a glass rod having a poly(tetrafluoroethylene) (PTFE) rotor blade at the end.

The synthesis of Ni nanoparticles was performed according to Scheme 1. Nickel formate dihydrate (5 mmol) and oleylamine (50 mmol) were mixed and then heated at 393 K for 10 min. The color of the reaction solution changed in the same way as the case of preparing the complex of $[Ni(HCOO)_2(C_{12}H_{25}NH_2)_2]$ described above, confirming the complexation of nickel formate with oleylamine ligands. After cooling to room temperature, 1-octanol (60 mL) was added to the solution. This solution in a quartz vessel was heated at a rate of 40 K min^{-1} under microwave irradiation and then left to stand at 463 K for 10 min under nitrogen atmosphere. The reaction solution was cooled to room temperature. The obtained particles were centrifuged and washed in methanol to remove the residual long-chain amines and dried under vacuum at 334 K for 4 h. Black Ni nanoparticles were obtained (denoted as A). Temperature profiles of this reaction with time and microwave (MW) power are shown in Figure S1 (Supporting Information). Nanoparticles using other long-chain amine ligands such as myristylamine and laurylamine were obtained under the same reaction conditions (denoted as B and C, respectively).

Instruments. Fourier transform infrared spectroscopy was applied to the nickel complexes in KBr pellets using a Perkin-Elmer 2000FT-IR spectrometer. UV–vis spectra were obtained using a V-570 spectrophotometer (JASCO Co.). The sizes and morphologies of Ni nanoparticles were characterized by a transmission electron microscope (TEM) at 200 kV with a Hitachi H-800 (Hitachi High-Technologies Co.). The crystal phase of the powder was analyzed by using a MultiFlex (Rigaku Co.) with a Cu Kα radiation source in the range of the 2θ Bragg angles = 20–90° at 40 kV and 40 mA. The amounts of surface modifying agents on the surface of Ni nanoparticles were determined by thermogravimetric analysis (TGA) using a Shimadzu TGA-50 analyzer. TGA was performed at a heating rate of 5 K min^{-1} in nitrogen atmosphere at a flow rate of 100 mL min^{-1}. Magnetic susceptibility data were obtained in various applied fields between −30 and 30 kOe by using a SQUID susceptometer (MPMS-5S, Quantum Design Co.).

Density Functional Theory (DFT) Calculation. DFT calculation was performed by using the Spartan' 06 program (Wavefunction, Inc. Irvine, CA). Fully optimized geometries were obtained for the Ni^{2+} complexes in the ground state at DFT B3LYP/6-31G** level. Electrostatic potential maps of the Ni^{2+} complexes in the ground state were obtained in the calculation for the obtained equilibrium geometry at the DFT B3LYP/6-31G** level.

Results

Microwave-Assisted Synthesis of Ni Nanoparticles from Nickel Formate Complex with Long-Chain Amine Ligands. The powder X-ray diffraction pattern of sample A is shown in

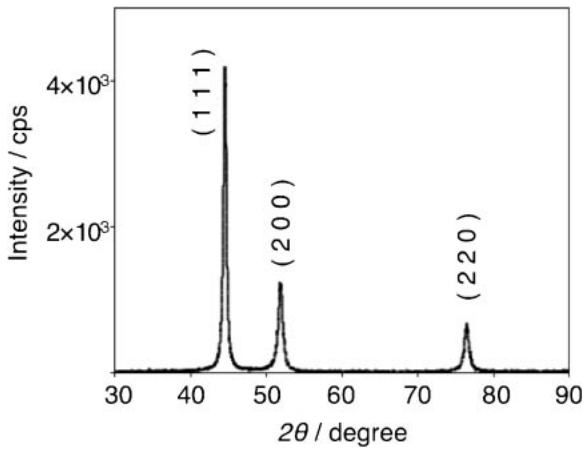

Figure 1. X-ray diffraction pattern of sample A.

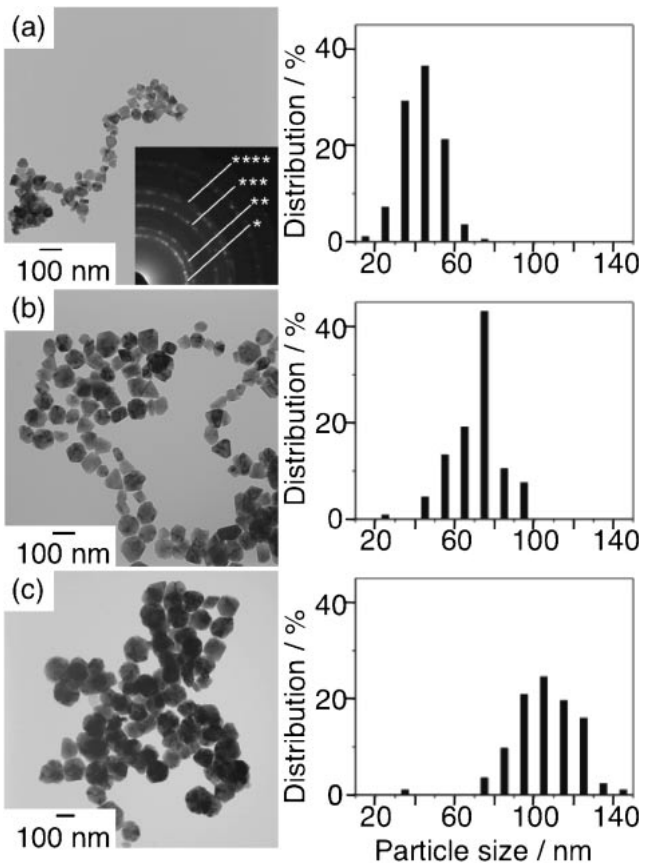

Figure 2. TEM images and particle size distributions of samples A (a), B (b), and C (c). Histograms of the size distributions of the samples were made by the diameters of randomly selected 200 particles. Inset of Figure 2a is the SAED pattern of the whole image of sample A. Debye rings are assigned to (111) (*), (200) (**), (220) (***), and (311) (****), respectively.

Figure 1. All the peaks of sample A produced by microwave irradiation were assigned to the pure phase of fcc Ni, including no other components such as NiO and Ni_3C and showing high crystallinity. The patterns of samples B and C showed the same fcc Ni diffraction patterns as well as that of sample A. The TEM images of samples A, B, and C are shown in Figure 2.

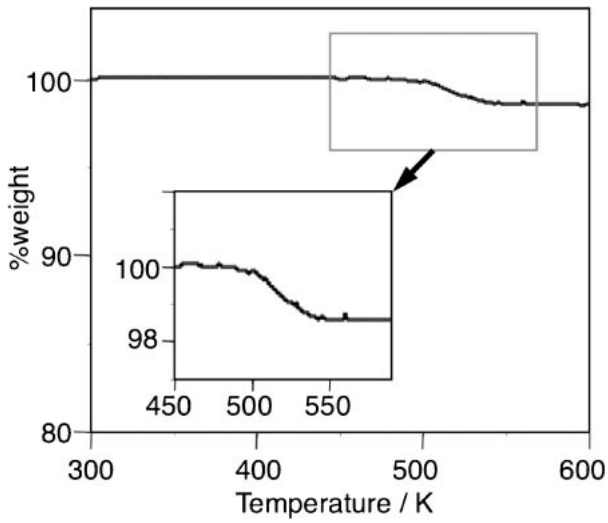

Figure 3. TGA measurement of sample A at a heating rate of 10 K min^{-1} under nitrogen flow of 100 mL min^{-1}.

The selected area electron diffraction (SAED) pattern of sample A (Figure 2a, inset) was a clear fcc Ni pattern. No ED pattern for NiO was observed. The average particle sizes were determined to be 43, 71, and 106 nm for samples A (oleylamine, $C_{18}H_{37}N$), B (myristylamine, $C_{14}H_{31}N$), and C (laurylamine, $C_{12}H_{27}N$), respectively, demonstrating that the particle sizes were controlled by changing the chain lengths of alkylamines under the same reaction conditions.

In order to determine the contents of the organic components on the surface of Ni nanoparticles, TGA measurements were carried out. Figure 3 shows the weight loss curve of sample A. The contents of the long-chain amines in samples A calculated on the basis of the weight loss were about 1.5 wt %. The contents of them in samples B and C were about 1.4 and 1.1 wt %, respectively. These results indicated that the small amounts of the long-chain amines were contained in the obtained powders. The amines remaining in the samples should be strongly adsorbed on the surface of the nanoparticles, since weakly adsorbed amines on the surface should be easily removed by the washing process.

For comparing with the above synthesis in the presence of amines, the nanoparticles were prepared by the reaction of nickel formate dihydrate (5 mmol) in tetraethylene glycol (60 mL) under microwave irradiation at 770 W at a heating rate of 40 K min^{-1} without adding amines and left to stand at 503 K for 10 min under nitrogen atmosphere. This experiment without addition of amines needed a temperature higher by 40 K due to the lack of reaction enhancement by adding amines and gave coarse particles with an average particle size of 250 nm (denoted as D), as shown in Figure 4a. Therefore, long-chain amines should act effectively as surface modifying agents to control the particle growth and to suppress aggregation in the reaction solution.

Ni nanoparticles were synthesized in tetraethylene glycol under the same reaction conditions as sample A using oleylamine (denoted as E). The TEM image of sample E is shown in Figure 4b. The particles were obtained as an agglomeration of 2–3 particles. Long chain alcohols seem suitable as solvents for preparing the monodispersed Ni nanoparticles.

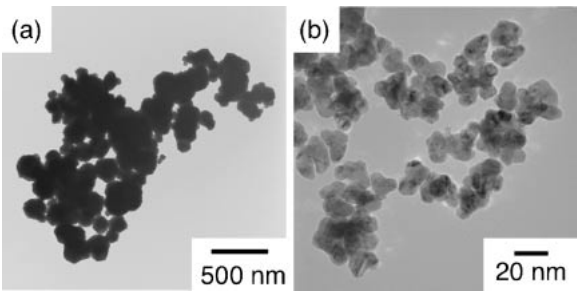

Figure 4. TEM images of samples D (a) and E (b).

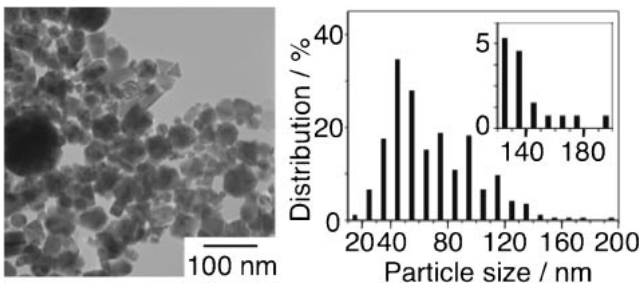

Figure 5. TEM image and particle size distribution of sample F. Histogram of the size distribution of sample F was made by measuring the diameters of randomly selected 200 particles.

Comparison of Microwave Heating with Conventional Heating. We examined the differences between the microwave-assisted method and the conventional method in the synthesis of Ni nanoparticles using oleylamine ligands. In the case of conventional heating, Ni nanoparticles were prepared in the same conditions except for the heating rate. The reaction solution was heated at a rate of ca. 5 K min^{-1} in an oil bath, which was the maximum rate available by heating with an oil bath. Although Ni nanoparticles were obtained (denoted as sample F), the resulting solution remained the blue color of the Ni^{2+} complex, indicating that the reaction did not proceed to completion. The yield Ni nanoparticles were 95.6% and 67% for the microwave-assisted method and the conventional method, respectively. The TEM image of sample F is shown in Figure 5. The average particle size was determined to be about 70 nm (standard deviation $\sigma = 32.5$ nm). Larger agglomerated particles were observed for the particles of sample F than those obtained under microwave irradiation (43 nm, $\sigma = 9.7$ nm). In the microwave-assisted method, the reaction solution was quickly and uniformly heated under microwave irradiation. Therefore, nucleus growth should simultaneously occur in the entire vessel and particles with a narrow size distribution should be obtained within a short time.[41–43]

Magnetic Properties. The magnetic properties of the Ni nanoparticles were carried out using a SQUID susceptometer. The temperature dependence of the magnetization of sample A between 10 and 400 K under various fields is shown in Figure 6. In the case of a zero-field-cooling (ZFC) process, the magnetization of the Ni nanoparticles under a 1000 Oe field increased with the rise in temperature. The magnetization reached the maximum point at 250 K, called the blocking temperature (T_B), and then decreased at temperatures above T_B. The magnetization plots in a field-cooling (FC) process under the same applied field showed different behaviors compared to those in a ZFC process. At temperatures above T_B, the plots in the FC process overlapped with those in the ZFC process. When the magnitude of the applied fields for the ZFC–FC process was varied from 100 to 500 and 1000 Oe, the blocking temperature shifted down from around 400 to 280 and 250 K, respectively. Magnetization versus the applied field plot at 300 K for sample A is shown in Figure 7. The average particle sizes, saturation magnetizations and coercive forces of samples A, B, and C are listed in Table 1. Sample A showed a saturation magnetization (σ_s) 43.7 emu g^{-1}, Samples B and C had higher σ_s ($\sigma_s = 48.8$ and 50.2 emu g^{-1}) than those of sample A, which was understandable taking the relationship of the average particle sizes of Ni nanoparticles into account.

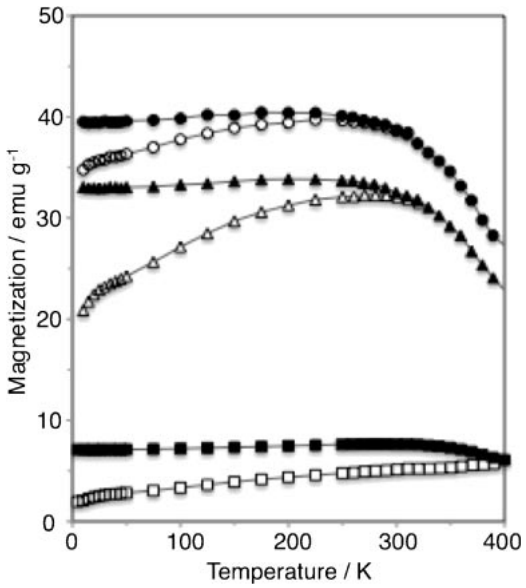

Figure 6. Temperature dependence of the magnetization for samples A (43 nm) in a ZFC and a FC process under various fields. [□(ZFC)–■(FC) plots at 100 Oe, △(ZFC)–▲(FC) plots at 500 Oe, and ○(ZFC)–●(FC) plots at 1000 Oe].

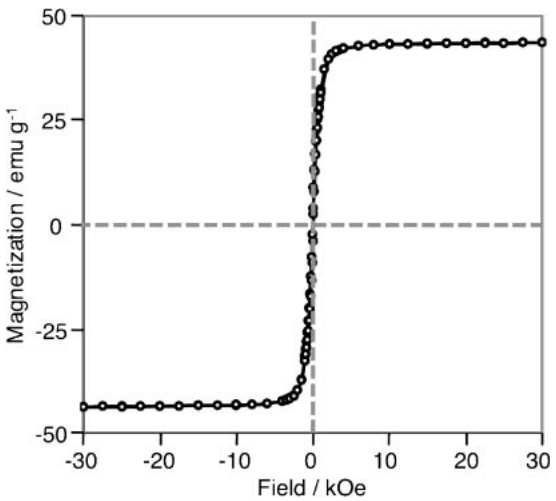

Figure 7. Magnetization versus applied fields for sample A at 300 K.

Table 1. The Particle Sizes, Coercive Forces H_c, and Saturation Magnetization σ_s of Samples A, B, and C at 300 K

	Particle size /nm	H_c/Oe	σ_s/emu g^{-1} at 30 kOe
Sample A	43	61	43.7
Sample B	71	55	48.8
Sample C	106	81	50.2

Discussion

The Formation of Nickel Formate Complexes with Long-Chain Amines. At the beginning of the synthetic process of Ni nanoparticles having laurylamine as a surface modifying agent according to Scheme 1, nickel formate dihydrate (5 mmol) and laurylamine (50 mmol) were heated at 393 K for 10 min in order to coordinate laurylamine to Ni^{2+} ion. The changes of the color of the solution and the UV–vis spectra of the precursor in solution were coincident with those observed in the preparation of the isolated complex ([Ni(HCOO)$_2$(C$_{12}$H$_{25}$NH$_2$)$_2$]), indicating the formation of a common species. Therefore, the properties of the precursor for the synthesis of Ni nanoparticles could be examined from those of the isolated [Ni(HCOO)$_2$(C$_{12}$H$_{25}$NH$_2$)$_2$]. We discussed the relationship between the intramolecular reduction at lower temperatures and the properties of the precursor with laurylamine ligands.

The composition of the isolated complex ([Ni(HCOO)$_2$(C$_{12}$H$_{25}$NH$_2$)$_2$]) was determined by elemental analysis. However, the geometric structure of the complex was not determined by X-ray structure analysis because a single crystal of the complex could not be obtained. Therefore, we examined the structure by FT-IR and UV–vis spectra.

Determination of Ligands Contained in [Ni(HCOO)$_2$(C$_{12}$H$_{25}$NH$_2$)$_2$] by FT-IR Spectra: Figure 8 shows the differences in the FT-IR spectra between nickel formate dihydrate itself and [Ni(HCOO)$_2$(C$_{12}$H$_{25}$NH$_2$)$_2$]. The spectrum of nickel formate dihydrate showed a peak at 1570 cm^{-1} attributed to the C=O asymmetric stretching vibration of formate ion, and a broad peak at 3100–3400 cm^{-1} attributed to the O–H stretching vibration of crystal water. In the case of [Ni(HCOO)$_2$(C$_{12}$H$_{25}$NH$_2$)$_2$], the peak of the O–H stretching vibration of crystal water disappeared. The sharp peaks at 2950–2850 and at 3325 and 3283 cm^{-1} were assigned to the stretching vibration of the aliphatic C–H group and the N–H asymmetric/symmetric stretching vibration of the laurylamine ligands, respectively. A sharp peak at 1620 cm^{-1} was assigned to the N–H bending vibration of the laurylamine ligands. It indicated that laurylamine ligands were coordinated to the Ni^{2+} ion. In addition, the shift of the C=O asymmetric stretching vibration to high wavenumber by ca. 15 cm^{-1} was observed for [Ni(HCOO)$_2$(C$_{12}$H$_{25}$NH$_2$)$_2$]. The result of the FT-IR spectra confirmed that the isolated complex ([Ni(HCOO)$_2$(C$_{12}$H$_{25}$NH$_2$)$_2$]) contained the ligands of formate ion and laurylamine. Furthermore, by considering both results of elemental analysis and FT-IR spectra, the structural formula of the isolated complex was determined to be [Ni(HCOO)$_2$(C$_{12}$H$_{25}$NH$_2$)$_2$].

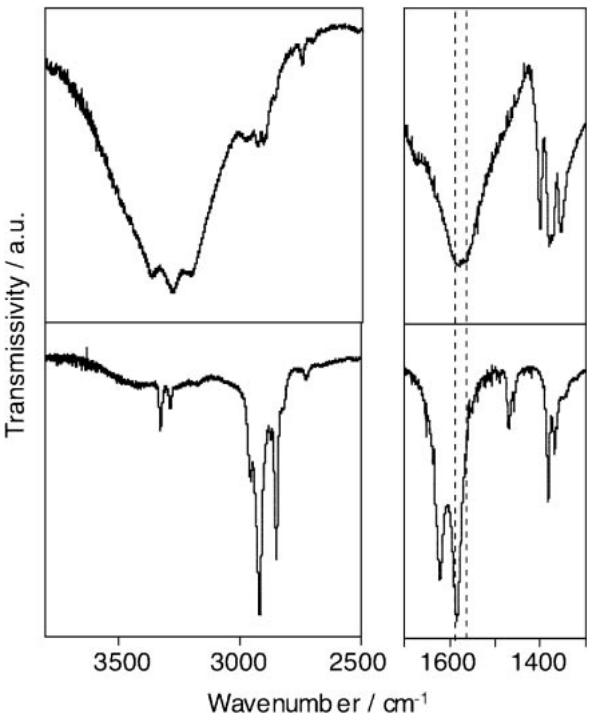

Figure 8. FT-IR spectra of nickel formate dihydrate (top) and [Ni(HCOO)$_2$(C$_{12}$H$_{25}$NH$_2$)$_2$] (bottom) in KBr pellets.

Determination of the Coordination Environment in [Ni(HCOO)$_2$(C$_{12}$H$_{25}$NH$_2$)$_2$] by UV–Vis Spectra: The coordination environments of Ni^{2+} complexes can be determined by comparing the three absorption bands of the first spin-allowed, the second spin-allowed, and the spin-forbidden d–d transitions ($^3A_2 \rightarrow {}^3T_2$, $^3A_2 \rightarrow {}^3T_1$, and $^3A_2 \rightarrow {}^1E$) with those of Ni^{2+} complexes having known structures. Figure 9 shows UV–vis spectra of nickel formate dihydrate in water and [Ni(HCOO)$_2$(C$_{12}$H$_{25}$NH$_2$)$_2$] in dichloromethane. The spectrum of nickel formate dihydrate closely resembled that of NiSO$_4$·6H$_2$O, showing that both complexes of nickel formate dihydrate and NiSO$_4$·6H$_2$O have the same coordination environment of six oxygen atoms (denoted as O_6 type). In contrast, the spectrum of [Ni(HCOO)$_2$(C$_{12}$H$_{25}$NH$_2$)$_2$] was different from both spectra of nickel formate dihydrate and NiSO$_4$·6H$_2$O. The first spin-allowed d–d transition band ($^3A_2 \rightarrow {}^3T_2$) of [Ni(HCOO)$_2$(C$_{12}H_{25}NH_2$)$_2$] shifted to high energy by ca. 664 cm^{-1} compared to that of nickel formate dihydrate (see Supporting Information Table S2). Meanwhile, the spectrum of [Ni(HCOO)$_2$(C$_{12}$H$_{25}$NH$_2$)$_2$] closely resembled that of [Ni(acac)$_2$(tmen)],[44–46] having the coordination environment of two nitrogen and four oxygen atoms (denoted as N_2O_4 type), (acac = acetylacetonato, tmen = *N*,*N*,*N*′,*N*′-tetramethylethylenediamine). Therefore, the similar spectra indicated that the complex of [Ni(HCOO)$_2$(C$_{12}$H$_{25}$NH$_2$)$_2$] had an N_2O_4 coordination environment. The results of elemental analysis, FT-IR, and UV–vis spectra made it clear that the isolated complex ([Ni(HCOO)$_2$(C$_{12}$H$_{25}$NH$_2$)$_2$]) was a six-coordinated complex composed of two bidentate formate ions and two monodentate laurylamines.

Long-chain amine providing a pair of electrons from the nitrogen at the end of an alkyl chain could be strongly

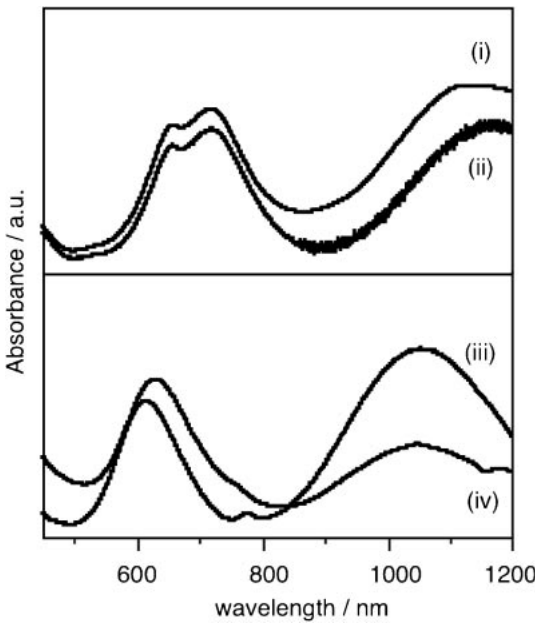

Figure 9. UV–vis spectra of nickel formate dihydrate (i), nickel sulfate hexahydrate (ii), [Ni(acac)$_2$(tmen)] (iii), and [Ni(HCOO)$_2$($C_{12}H_{25}NH_2$)$_2$] (iv) in water (top) and dichloromethane (bottom), respectively (acac = acetylacetonato, tmen = *N*,*N*,*N*′,*N*′-tetramethylethylenediamine).

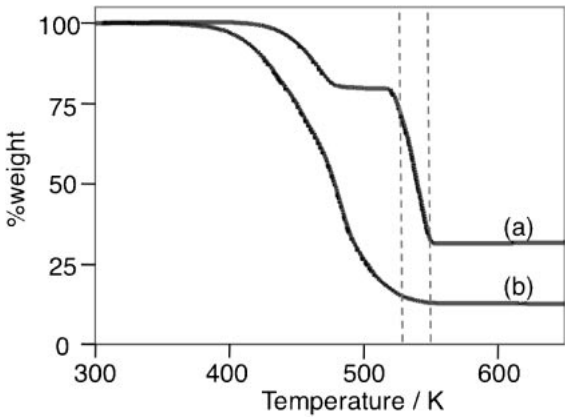

Figure 10. TGA measurement of nickel formate dihydrate (a) and [Ni(HCOO)$_2$($C_{12}H_{25}NH_2$)$_2$] (b) at a heating rate of 10 K min^{-1} under a nitrogen flow of 100 mL min^{-1}.

coordinated with Ni^{2+} ion to form the octahedral Ni^{2+} complex. Furthermore, the amine could convert very insoluble nickel formate dihydrate into a soluble complex. As a result, the unagglomerated particles were obtained by preparing in homogeneous solution.

Low-Temperature Thermal Decomposition of Formate Ion in the Ni^{2+} Complex with Long-Chain Amine Ligands. Experimental Evidence for Low-Temperature Thermal Decomposition: Figure 10 shows the weight loss curves of nickel formate dihydrate and [Ni(HCOO)$_2$($C_{12}H_{25}NH_2$)$_2$] under nitrogen atmosphere in TGA measurements. The thermal decomposition of nickel formate dihydrate consisted of two stages. The first weight loss (20.2 wt %) observed at 410–480 K could be attributed to dehydration (the theoretical value, 19.5 wt %). The second weight loss (48.5 wt %) observed at 520–553 K was attributed to the decomposition of formate ion (the theoretical value, 48.7 wt %). The residual weight content (31.4 wt %) corresponded to the theoretical Ni content (31.8 wt %) in nickel formate dihydrate.

Nickel powder was formed according to the following.[32–34]

$$Ni(HCOO)_2 \cdot 2H_2O \rightarrow Ni(HCOO)_2 + 2H_2O \quad (2)$$

$$Ni(HCOO)_2 \rightarrow Ni^0 + 2CO_2 \uparrow + H_2 \uparrow \quad (3)$$

In the case of [Ni(HCOO)$_2$($C_{12}H_{25}NH_2$)$_2$], the weight (87.3 wt %) continuously decreased up to 530 K. The residual weight (12.7 wt %) corresponded approximately to the theoretical Ni content (11.6 wt %). The decomposition temperature, at which the organic molecules in [Ni(HCOO)$_2$($C_{12}H_{25}NH_2$)$_2$] were removed and only Ni^0 remained, was lower by 23 K than that of nickel formate dihydrate. These results indicated that long-chain amine ligands coordinated to Ni^{2+} ion enhanced the decomposition of formate ion and decreased the energy required for the intramolecular reduction of nickel formate complexes.

Effect of Ligation of the Long-Chain Amines on the Decomposition of the Nickel Formate Complex: The formate ion is ordinarily stabilized by the counter cation (Ni^{2+} ion). Therefore, diminishment of the binding power between Ni^{2+} and formate ions is required for decomposition at lower temperatures. The lengthening of the bond distance of Ni–O(formate ligand) in the Ni^{2+} complex is needed for the reaction at lower temperatures because the bond energy of Ni–O(formate ligand) is decreased by increase of the bond distance.

Baba and Yasuda et al. have reported that bromide coordination to tin enolate increases the nucleophilicity and decreased Lewis acidity of the metal center promoting the reaction of enolate ligand with organic halide.[47,48] The coordination of halide ligand as an electron donor to the tin enolate complex increased the electron density the metal center and the bond distance of Sn–O(enolate ligand). Their observation led to an idea that the coordination of the electron-donating ligands to nickel formate complex increased the electron density of Ni^{2+} ion and the bond distance of Ni–O(formate ligand). Ivaniková et al. have succeeded in preparation of nickel formate complexes containing N-donor base ligands and reported that the coordination of imidazole ligands increased the distance of Ni–O(formate ligand).[49] Now, the effect of long-chain amine ligands as N-donor base ligands on the nickel formate complexes can be understood as increasing the distance of Ni–O(formate ligand) and lowering the decomposition temperature of the formate complex. We have calculated the bond distance of Ni–O(formate ligand) of the nickel formate complexes by DFT calculation.

DFT Studies of the Structures of the Nickel Complexes. The DFT calculations were carried out to estimate the charge densities and the bond distances of Ni–L(ligand) in both [Ni(HCOO)$_2$($C_{12}H_{25}NH_2$)$_2$] and nickel formate dihydrate. The three-dimensional electrostatic potential views and the structures of both complexes obtained by the DFT calculations at the B3LYP/6-31-G** level are depicted in Figure 11. The bond distances obtained from the DFT calculations are listed in Table 2. As shown in Figure 11, there was a large difference in

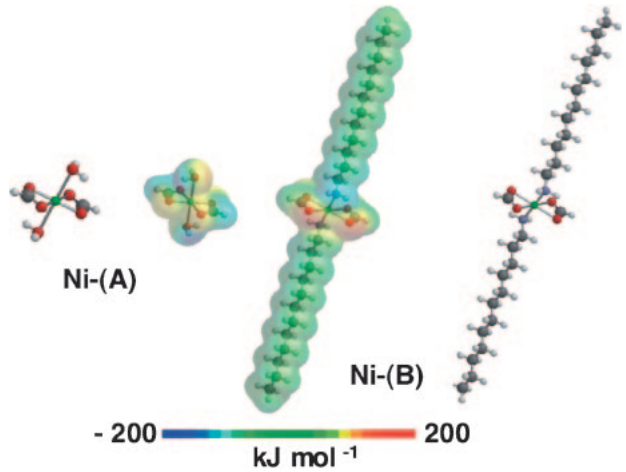

Figure 11. Three-dimensional electrostatic potential views and structures obtained by DFT calculations at the B3LYP/6-31-G** level. Ni-(A) nickel formate dihydrate, Ni-(B) $[Ni(HCOO)_2(C_{12}H_{25}NH_2)_2]$ complex. Electrostatic potential map from −200 to 200 kJ mol^{-1} onto a 0.002 eÅ^{-3}.

Table 2. Bond Lengths/Å and Angles/° of the Complexes Ni-(A) and Ni-(B) Obtained by the DFT Calculations

	Ni-(A)	Ni-(B)
Ni–O(formate)	1.944	2.267
C–O(formate)	1.271	1.262
O–Ni–O(formate)	68.00	58.88

the electrostatic potential between $[Ni(HCOO)_2(C_{12}H_{25}NH_2)_2]$ and nickel formate dihydrate. The charges of the four oxygen atoms (−0.679) of the two formate ligands ($[Ni(HCOO)_2(C_{12}H_{25}NH_2)_2]$) were more negative than those (−0.499) of nickel formate dihydrate. Furthermore, the distances of Ni–O(formate ligand) (2.267 Å) in $[Ni(HCOO)_2(C_{12}H_{25}NH_2)_2]$ were much longer than those of Ni–O(formate ligand) (1.944 Å) in nickel formate dihydrate. These results indicated that the coordination of long-chain amine ligands as electron donors to Ni^{2+} complexes containing formate ligands increased the electron density of the metal center and the bond distance of Ni–O(formate ligands). Therefore, the DFT calculations confirmed the enhancement of long-chain amine ligands attached to Ni^{2+} ion on the reductive decomposition of the nickel formate complex giving Ni nanoparticles.

Conclusion

In summary, we have succeeded in rapid preparation of monodisperse Ni nanoparticles by the intramolecular reduction of Ni^{2+} contained in a formate complex with long-chain amine ligands under microwave irradiation. The low-temperature decomposition of the formate ion was realized by the coordination of electron-donating ligands to nickel formate complex, and then the Ni nanoparticles could be obtained at low temperatures. The particle sizes were controlled using several long-chain amine ligands.

This work supported financially by Nippon Steel Chemical Co., Ltd., Japan and Iwatani International Co., Ltd., Japan. We thank Dr. T. Sakata and Prof. H. Mori, Research Center for Ultra-High Voltage Electron Microscopy, Osaka University and Ms M. Takahashi at Wavefunction, Inc. Irvine, CA for supporting DFT calculation.

Supporting Information

Time profiles of temperature and MW power in the synthesis of sample A and a table of the absorption energies of Ni complexes. This material is available free of charge on the web at http://www.csj.jp/journals/bcsj/.

References

1 G. Schmid, *Chem. Rev.* **1992**, *92*, 1709.
2 K. R. Gopidas, J. K. Whitesell, M. A. Fox, *Nano Lett.* **2003**, *3*, 1757.
3 D. J. Maxwell, J. R. Taylor, S. Nie, *J. Am. Chem. Soc.* **2002**, *124*, 9606.
4 P. V. Kamat, *J. Phys. Chem. B* **2002**, *106*, 7729.
5 T. K. Sau, C. J. Murphy, *J. Am. Chem. Soc.* **2004**, *126*, 8648.
6 M.-C. Daniel, D. Astruc, *Chem. Rev.* **2004**, *104*, 293.
7 M. M. Oliveira, E. G. Castro, C. D. Canestraro, D. Zanchet, D. Ugarte, L. S. Roman, A. J. G. Zarbin, *J. Phys. Chem. B* **2006**, *110*, 17063.
8 S. Sun, C. B. Murray, D. Weller, L. Folks, A. Moser, *Science* **2000**, *287*, 1989.
9 W. X. Zhang, C. B. Wang, H. L. Lien, *Catal. Today* **1998**, *40*, 387.
10 D. V. Leff, P. C. Ohara, J. R. Heath, W. M. Gelbart, *J. Phys. Chem.* **1995**, *99*, 7036.
11 C. Burda, X. Chen, R. Narayanan, M. A. El-Sayed, *Chem. Rev.* **2005**, *105*, 1025.
12 M. Tsuji, R. Matsuo, P. Jiang, N. Miyamae, D. Ueyama, M. Nishio, S. Hikino, H. Kumagae, K. S. N. Kamarudin, X.-L. Tang, *Cryst. Growth Des.* **2008**, *8*, 2528.
13 M. G. Perichaud, J. Y. Deletage, H. Fremont, Y. Danto, C. Faure, M. Salagoity, *IEEE, International Electronics Manufacturing Technology Symposium* **1998**, p. 377.
14 T. R. Rao, *Fundamentals of Microsystem Packaging*, McGraw Hill International Edition, **2001**.
15 W. Chen, L. Li, J. Qi, Y. Wang, Z. Gui, *J. Am. Ceram. Soc.* **1998**, *81*, 2751.
16 N. Sato, H. Katayama, S. Ogasawara, *Kawasaki Seitetsu Giho* **2002**, *34*, 120.
17 Y. Koltypin, A. Fernandez, T. C. Rojas, J. Campora, P. Palma, R. Prozorov, A. Gedanken, *Chem. Mater.* **1999**, *11*, 1331.
18 D.-H. Chen, S.-H. Wu, *Chem. Mater.* **2000**, *12*, 1354.
19 S.-H. Wu, D.-H. Chen, *Chem. Lett.* **2004**, *33*, 406.
20 O. Margeat, C. Amiens, B. Chaudret, P. Lecante, R. E. Benfield, *Chem. Mater.* **2005**, *17*, 107.
21 M. Green, P. O'Brien, *Chem. Commun.* **2001**, 1912.
22 Y. Hou, S. Gao, *J. Mater. Chem.* **2003**, *13*, 1510.
23 H. Winnischofer, T. C. R. Rocha, W. C. Nunes, L. M. Socolovsky, M. Knobel, D. Zanchet, *ACS Nano* **2008**, *2*, 1313.
24 L. K. Kurihara, G. M. Chow, P. E. Schoen, *Nanostruct. Mater.* **1995**, *5*, 607.
25 N. Chakroune, G. Viau, C. Ricolleau, F. Fiévet-Vincent, F. Fiévet, *J. Mater. Chem.* **2003**, *13*, 312.
26 G. M. Chow, J. Ding, J. Zhang, K. Y. Lee, D. Surani, S. H. Lawrence, *Appl. Phys. Lett.* **1999**, *74*, 1889.
27 H. Yin, G. M. Chow, *J. Electrochem. Soc.* **2002**, *149*, C68.

28 P. Toneguzzo, G. Viau, O. Acher, F. Guillet, E. Bruneton, F. Fievet-Vincent, F. Fievet, *J. Mater. Sci.* **2000**, *35*, 3767.
29 C. N. Chinnasamy, B. Jeyadevan, K. Shinoda, K. Tohji, A. Narayanasamy, K. Sato, S. Hisano, *J. Appl. Phys.* **2005**, *97*, 10J309.
30 Z. Zhang, X. Chen, X. Zhang, C. Shi, *Solid State Commun.* **2006**, *139*, 403.
31 V. Rosenband, A. Gany, *J. Mater. Process. Technol.* **2004**, *153–154*, 1058.
32 P. G. Fox, J. Ehretsmann, C. E. Brown, *J. Catal.* **1971**, *20*, 67.
33 E. Iglesia, M. Boudart, *J. Catal.* **1984**, *88*, 325.
34 A. B. Edwards, C. D. Garner, K. J. Roberts, *J. Phys. Chem. B* **1997**, *101*, 20.
35 J.-H. Lee, C.-K. Kim, S. Katoh, R. Murakami, *J. Alloys Compd.* **2001**, *325*, 276.
36 F. Bondioli, A. M. Ferrari, C. Leonelli, C. Siligardi, G. C. Pellacani, *J. Am. Ceram. Soc.* **2001**, *84*, 2728.
37 M. N. Nadagouda, R. S. Varma, *Cryst. Growth Des.* **2008**, *8*, 291.
38 T. Yamamoto, Y. Wada, T. Sakata, H. Mori, M. Goto, S. Hibino, S. Yanagida, *Chem. Lett.* **2004**, *33*, 158.
39 T. Nakamura, Y. Tsukahara, T. Sakata, H. Mori, Y. Kanbe, H. Bessho, Y. Wada, *Bull. Chem. Soc. Jpn.* **2007**, *80*, 224.
40 T. Nakamura, Y. Tsukahara, T. Yamauchi, T. Sakata, H. Mori, Y. Wada, *Chem. Lett.* **2007**, *36*, 154.
41 Y. Wada, H. Kuramoto, T. Sakata, H. Mori, T. Sumida, T. Kitamura, S. Yanagida, *Chem. Lett.* **1999**, 607.
42 M. Tsuji, M. Hashimoto, T. Tsuji, *Chem. Lett.* **2002**, 1232.
43 D. Li, S. Komarneni, *J. Am. Ceram. Soc.* **2006**, *89*, 1510.
44 Preparation of the Ni^{2+} complex $[Ni(acac)_2(tmen)]$; Crystalline $[Ni(acac)_2(tmen)]$ was prepared in the following procedure.[45,46] An aqueous solution of nickel dichloride (12 mmol) was mixed with acetylacetone (24 mmol) and an aqueous solution of potassium hydroxide (24 mmol). The resulting solution was stirred for 10 min. Then tmen (15 mmol) was added into the mixture and the solution was stirred for 20 min. The complex was extracted with 1,2-dichloromethane and purified by recrystallizing from 1,2-dichloromethane under air atmosphere.
45 T. Yoshida, T. Suzuki, K. Kanamori, S. Kaizaki, *Inorg. Chem.* **1999**, *38*, 1059.
46 S. Kaizaki, T. Yamauchi, *Inorg. Chim. Acta* **2007**, *360*, 649.
47 M. Yasuda, K. Chiba, A. Baba, *J. Am. Chem. Soc.* **2000**, *122*, 7549.
48 M. Yasuda, K. Chiba, N. Ohigashi, Y. Katoh, A. Baba, *J. Am. Chem. Soc.* **2003**, *125*, 7291.
49 R. Ivaniková, R. Boča, L. Dlháň, H. Fuess, A. Mašlejová, V. Mrázová, I. Svoboda, J. Titiš, *Polyhedron* **2006**, *25*, 3261.